Spironolactone ameliorates lipopolysaccharide-induced cholestasis in rats by improving Mrp2 function: Role of transcriptional and post-transcriptional mechanisms

María Valeria Razori, Pamela L. Martín, Paula M. Maidagan, Ismael R. Barosso, Nadia Ciriaci, Romina B. Andermatten, Enrique J. Sánchez Pozzi, Cecilia L. Basiglio, María Laura Ruiz, Marcelo G. Roma

PII: S0024-3205(20)31105-X

DOI: https://doi.org/10.1016/j.lfs.2020.118352

Reference: LFS 118352

To appear in: *Life Sciences*

Received date: 11 June 2020

Revised date: 14 August 2020

Accepted date: 24 August 2020

Please cite this article as: M.V. Razori, P.L. Martín, P.M. Maidagan, et al., Spironolactone ameliorates lipopolysaccharide-induced cholestasis in rats by improving Mrp2 function: Role of transcriptional and post-transcriptional mechanisms, *Life Sciences* (2020), https://doi.org/10.1016/j.lfs.2020.118352

Spironolactone ameliorates lipopolysaccharide-induced cholestasis in rats by improving Mrp2 function: Role of transcriptional and post-transcriptional mechanisms

María Valeria Razori, Pamela L. Martín, Paula M. Maidagan, Ismael R. Barosso, Nadia Ciriaci, Romina B. Andermatten, Enrique J. Sánchez Pozzi, Cecilia L. Basiglio, María Laura Ruiz*, Marcelo G. Roma*

Institute of Experimental Physiology (IFISE)

Faculty of Biochemical and Pharmaceutical Sciences of the National University of Rosario, 2000-Rosario, ARGENTINA

*These authors contributed equally to this work.

Author for correspondence:

Marcelo G. Roma, Ph.D.

Institute of Experimental Physiology (IFISE)

Facultad de Ciencias Bioquímicas y Farmacéuticas

Suipacha 570, 2000 – Rosario, ARGENTINA

Tel.: +54-341-4305799

Fax: +54-341-4399473

E-mail: mroma@fbioyf.unr.edu.ar

Abstract

Aims: Lipopolysaccharide (LPS) induces inflammatory cholestasis by impairing expression, localization, and function of carriers involved in bile formation, e.g. bile salt export pump (Bsep) and multidrug resistance associated protein 2 (Mrp2). A specific therapy against this disease is still lacking. Therefore, we evaluated the anticholestatic effects of spironolactone (SL), a PXR ligand that regulates bile salt homeostasis, up-regulates Mrp2, and bears anti-inflammatory properties.

Main methods: Male Wistar rats were divided into four groups: Control, SL (83.3 mg/kg/day of SL, i.p., for 3 days), LPS (2.5 mg/kg/day, i.p., at 8 am of the last 2 days, and 1.5 mg/kg/day at 8 pm of the last day), and SL+LPS. Biliary and plasma parameters and the expression, function and localization of Mrp2 and Bsep were evaluated.

Key findings: SL partially prevented LPS-induced drop of basal bile flow by normalizing the bile salt-independent fraction of bile flow (BSIBF), via improvement of glutathione output. This was due to a recovery in Mrp2 transport function, the major canalicular glutathione transporter, estimated by monitoring the output of its exogenously administered substrate dibromosulfophthalein. SL counteracted the LPS-induced downregulation of Mrp2, but not that of Bsep, at both mRNA and protein levels. LPS induced endocytic internalization of both transporters, visualized by immunofluorescence followed by confocal microscopy, and SL partially prevented this relocalization. SL did not prevent the increase in IL-1β, IL-6, and TNF-α plasma levels.

Significance: SL prevents the impairment in Mrp2 expression and localization, and the

resulting recovery of Mrp2 function normalizes the BSIBF by improving glutathione excretion.

Keywords: Spironolactone; hepatocellular transporters; multidrug resistance-associated protein 2; lipopolysaccharide-induced cholestasis.

Abbreviations: ALP, alkaline phosphatase; ALT, alanine aminotransferase; AST, aspartate aminotransferase; AUC, area under the curve; BF, bile flow; BS, bile salts; Bsep, bile salt export pump; BSIBF, bile salt-independent fraction of bile flow; DBSP, dibromosulfophthalein; GSH, glutathione; JNK, c-jun-NH2-terminal kinase; LDH, lactate dehydrogenase; LPS, lipopolysaccharide; Mrp2, multidrug resistance-associated protein 2; Mrp3, multidrug resistance-associated protein 3; PXR, pregnane X receptor; RXRα, 9-cis-retinoic acid receptor-α; SL, spironolactone; TBA, total bile acids; TC, taurocholate; UDCA, ursodeoxycholic acid.

1. Introduction

Sepsis-induced cholestasis is a prototypical inflammatory cholestasis [1]. It is caused by the impairment in bile production induced by lipopolysaccharide (LPS) of the bacterial wall (endotoxins), and the subsequent release of pro-inflammatory cytokines [2]. The classic clinical case of sepsis-induced cholestasis is an icteric patient with a Gram (-) bacteremia, hospitalized in an intensive care unit. Patients undergoing septic shock may develop liver failure [3]. Among the multi-organ failures involved in sepsis, liver dysfunction is of remarkable prognostic importance for the clinical course, since it is a strong independent predictor of mortality, and therefore, its prevention has become imperative [4].

Inflammatory cholestasis involves primary alterations in bile formation, generally associated with transcriptional and post-transcriptional alterations in the expression and/or localization of hepatocellular carriers [5,6]. The canalicular transfer of bile salts (BS) by the bile salt export pump (Bsep/Abcb11) and of bilirubin glucuronide/glutathione (GSH) by the multidrug resistance-associated protein 2 (Mrp2/Abcc2) is the rate-limiting step in the overall transport from plasma to bile for these compounds. The expression of Bsep and Mrp2 is decreased in sepsis-induced cholestasis [7]. Transcriptional alterations of these carriers are mainly due to the repressed expression of nuclear receptors, such as pregnane X receptor (PXR) [8]. Inflammatory cholestasis also causes short-term, post-translational deleterious effects on canalicular transporter localization. Indeed, Mrp2 and Bsep undergo endocytic internalization in endotoxemia [9].

In a previous work [10], we studied the anti-cholestatic effects of ursodeoxycholic acid (UDCA) in LPS-induced cholestasis, as it is the “first choice” therapeutic approach for most cholestatic hepatopathies. Since its beneficial effects were partial, we decided to evaluate spironolactone (SL) as a complementary anti-cholestatic agent, which could act via alternative pathways. SL is a medicine used as a diuretic agent to reduce high blood pressure and edema, and for the treatment of heart failure [11]. It is also a transactivating ligand of the nuclear receptor PXR [12,13], a transcription factor that up regulates Mrp2 expression and regulates genes involved in BS homeostasis, which could be beneficial in this kind of cholestasis [14]. Modulating effects of SL on bile secretion have been described, as a result of increments in Mrp2 expression and the consequent higher secretion of GSH, a main driving force of the so called bile salt-independent fraction of bile flow (BSIBF) [15]. In addition, beneficial effects of SL in a model of non-inflammatory cholestasis in rodents induced by ethynylestradiol have been described [16]; a similar anticholestatic effect in an inflammatory model of cholestasis cannot be however inferred, since both kinds of cholestasis involves a differential subset of nuclear receptors [8], and are triggered by dissimilar signaling mechanisms [9]. Finally, anti-inflammatory properties of PXR have also been reported [17,18], and this could be particularly relevant for inflammatory hepatopathies like the one we are studying here.

Since there have been no studies to date showing that SL is able to counteract some of the alterations that occur in inflammatory cholestasis, in this study we evaluated the effect of SL on LPS-induced cholestasis, and the underlying mechanisms involved in its beneficial effects.

2. Materials and methods

2.1. Chemicals

LPS from Salmonella typhimurium, SL, NADPH, and GSH reductase were purchased from Sigma-Aldrich (St. Louis, MO). Sodium taurocholate (TC) was purchased from Santa Cruz Biotechnology (Dallas, Texas, U.S.A.). Dibromosulfophthalein (DBSP) was obtained from the Société d´Etudes et de Recherche Biologique (Paris, France). All other chemicals were of analytical grade purity, and used as supplied.

2.2. Animals and treatments

Adult male Wistar rats (90 days), weighing 300-350 g, were used. They were obtained from the Center for Comparative Medicine, Institute of Veterinary Sciences of Litoral, UNL-CONICET. Animals were maintained with a standard diet, water and saline solution ad libitum, under a constant 12 h-light/12 h-dark cycle. During the experiments, vital signs (heart rate and respiratory rate) and pain sensitivity were monitored. All treatments and animal experiments were carried out in the Institute of Experimental Physiology (IFISE). Animals received humanitarian care according to, the "Guide for the care and use of laboratory animals" published by the National Institutes of Health (NIH Publications No. 8023, revised 1978) and the ARRIVE (Animal Research: Reporting In Vivo Experiments) guidelines (http://www.nc3rs.org/ARRIVE). Animal experiments were approved by the Bioethics Committee for the Care and Use of Laboratory Animals of the Faculty of Biochemical and Pharmaceutical Sciences of the National University of

Rosario (Resolution No. 489/2015).

Rats were randomized in the following four experimental groups:

LPS group: Animals were injected with SL vehicle (corn oil i.p. at a daily dose of 5.85 ml/kg of b.w. and 6% DMSO), for 3 consecutive days. Animals also received 3 LPS doses, as follows: at 8:00 am of the last two days, the animals were given a single, i.p. injection of LPS of Salmonella typhimurium (2.5 mg/kg/day of b.w., dissolved in saline) and, at 8:00 pm of the last day, a third dose of LPS of 1.5 mg/kg of b.w. was injected. Due to the high variability of LPS dosage to induce cholestasis in the literature, this treatment protocol was established in ancillary experiments where different dosages were tested, aimed to obtain consistent drops in bile flow with minimal side effects.

SL group: Animals were injected with SL, i.p., at a dose of 83.3 mg/kg of b.w., dissolved in corn oil and 6% DMSO, for 3 days. At this dosage, we showed that SL induces both choleresis to untreated rats [15] and anti-cholestatic effects in rats treated with ethynyl estradiol [16].

SL + LPS group: Animals were injected with SL and with 3 LPS doses, as indicated in the previous groups.

Control group: Animals were injected only with LPS and SL vehicles.

Rats were provided with saline solution to drink “ad libitum” to compensate possible excess of NaCl loss due to SL diuretic effects. Since, according to set-up, ancillary experiments where the saline consumed was measured, endotoxemic, SL-treated

animals drunk approx. 3 ml or 6 ml in average less saline depending on their lethargic state (over or subtle), they received additionally one or two daily subcutaneous injections of saline solution of 3 ml each.

2.3. Surgical procedures

After the treatments were completed, and 12 hs after the last dose of LPS, animals were anesthetized with ketamine/xylazine (100 mg/kg of b.w. and 3 mg/kg of b.w., i.p., respectively), and thus maintained throughout the experiment. Body temperature was monitored with a rectal probe, and maintained between 36 and 37.5 °C with a heating lamp. Then, the common bile duct and the femoral vein were cannulated with PE10 and PE50 polyethylene tubing, respectively (Intramedic, Clay Adams, Parsippany, NJ) to collect bile samples and carry out transporter functionality estimations. At the end of the experiments, the animals were euthanized by exsanguination, and blood and liver samples were collected for further studies.

2.4. Bile and plasma samples collection and analytical procedures

Bile samples were collected for 10 min to monitor basal bile flow (BF), which was determined gravimetrically assuming a density of 1 g/ml. Basal bile was assayed for both total bile acids (TBA) and GSH, the two main biliary solutes acting as driving force for bile formation [19]. TBA in bile were measured by using the commercial kit RANDOX Laboratories Limited (Crumlin, United Kindom) (TBA, 5th generation, enzymatic colorimetric assay), whereas total GSH content was assessed by using the recycling

method of Tietze [20], as modified by Griffith [21]. Once finished the bile collection period, animals were euthanized by exsanguination, and the liver removed. In order to evaluate the degree of the hepatic injury, plasma samples were assayed for alkaline phosphatase (ALP; EC 3.1.3.1), aspartate aminotransferase (AST; EC 2.6.1.1), alanine aminotransferase (ALT; EC 2.6.1.2), and lactate dehydrogenase (LDH; EC. 1.1.1.27) by using a CM250 Autoanalyzer (Wiener Lab, Rosario, Argentina).

A blood sample from the tail vein was also obtained 2 h after the second LPS injection, to measure plasma levels of the inflammatory cytokines IL 1-β, IL-6 and TNF-α, by using commercial kits (IL-1 beta Rat ELISA Kit, IL-6 Rat ELISA Kit, TNF alpha Rat ELISA Kit from Invitrogen, Waltham, Massachusetts, USA).

2.5. Biliary excretion of exogenous Mrp2 and Bsep substrates

The time-course of the changes in the biliary output of the exogenously administered Bsep and Mrp2 solutes TC [19] and DBSP [22], respectively, have been assessed to estimate in vivo the transport efficiency of these canalicular carriers. Despite uptake of these solutes may be affected by LPS treatment [23], this process is unlikely to significantly influence biliary excretion, because *1*) canalicular transfer but not basolateral uptake is the rate-limiting step in the hepatic handling of cholephilic compounds [24], and *2*) kinetic studies suggest that the ABC canalicular transporters work under *T*m conditions [25], so that changes in intracellular levels due to impaired uptake should have negligible, if any effect on biliary excretion; this situation is unlikely

to be modified by LPS, because canalicular excretion is impaired to a similar or even higher extent than uptake by endotoxin [26].

TC, a model BS that is excreted into the canalicular lumen by Bsep [27], was injected at a single, i.v. dose of 8 μmol/100 g b.w. [10]. Then, bile samples were collected every 2 min for 10 min. According to ancillary experiments, after this time period, the exogenously administered TC has been completely cleared in control animals (data not shown). Therefore, TBA were measured in bile, and TC excretion was calculated by assuming that all the excess in biliary excretion rate of TBA over the basal one after TC injection is fully due to TC excretion, as shown elsewhere [10].

Mrp2 functionality was estimated by using DBSP, since this dye excreted into the canalicular lumen by this transporter after having been taken up by the hepatocyte by the organic anion-transporting polypeptide [22]; DBSP is not conjugated within the hepatocyte [28], and therefore its biliary excretion is independent on the changes in conjugation enzyme levels induced by SL [29]. To carry out the study, DBSP was administered at a single, i.v. dose of 15 mg/kg of b.w. Bile samples were then collected in 5-min intervals over the next 60 min, a time period long enough to virtually fully depurate the dye in control animals (data not shown). DBSP in bile was determined by spectrophotometry at a wavelength of 580 nm, after appropriate dilution with 0.1 N NaOH [30].

2.6. Assessment of BSIBF

Since BS are osmotic entities capable of stimulating bile formation, there is a direct and linear relationship between BF and TBA output [31], as follows:

BF = m.TBA output + h

Where:

m = Choleretic efficiency of BS.

h = BSIBF

To obtain the parameters of this equation, a bolus of TC was administered i.v. at the dose of 8 µmol/100 g of b.w., and bile was collected every 2 min for 10 min. TBA were measured in bile and the TBA output was calculated as previously indicated above. BF *vs.* TBA output values were plotted, and a linear regression curve was fitted for each set of values, with y-intercept and slope being BSIBF and choleretic efficiency, respectively.

2.7. Bsep and Mrp2 protein expression

Western blot analyses of Bsep and Mrp2 in total homogenate and fractions enriched in canalicular membrane proteins were performed as described previously [32]. Then, samples were loaded on polyacrylamide gels under denaturing conditions, and then subjected to electrophoresis. Once the electrophoresis was completed, proteins were transferred from the gel to PVDF membranes. Subsequently, the membranes were removed and blocked with buffer (50 ml PBS 1X, Tween 0.3% and 5 g of low fat dry milk) for at least 1 h. After blocking, they were incubated with the primary antibodies overnight at 4 °C (monoclonal mouse anti-rat Mrp2 antibody, 1:1000, M2 III-6, Alexis

Biochemicals, Carlsbad, CA; or polyclonal rabbit anti-rat Bsep antibody, 1:1000, Anti-SPGP pAb, Kamiya Biomedical Company, Seattle, WA USA). The next day, the membranes were washed, and immune complexes were detected by incubation with horseradish peroxidase linked to secondary antibodies for 1 h. Immunoreactive bands were detected using a bioluminescent reagent (ECL, Amersham Pharmacia Biotech, Inc). Membranes were re-probed with an anti-β actin antibody as loading control (Sigma–Aldrich Corp). Subsequently, the bands were quantified by densitometry, using the Gel Pro Analyzer Software (Media Cybernetics, Silver Spring, MD).

2.8. Real-time PCR study of Bsep and Mrp2

Total RNA was isolated from liver tissue using TRIzol® reagent (Invitrogen), according to manufacturer's instructions. Yield, purity, and integrity of RNA were assessed. Then, the first strand cDNA was synthesized using Superscript III Reverse Transcriptase and random primers (Invitrogen), according to the manufacturer's suggested protocol. Sequences of primer pairs and conditions for Mrp2, Bsep, and 18S were as previously described [10,16] (Table 1). Real-time PCR reactions were carried out in a Mx3000P System (Stratagene, La Jolla, CA) with Platinum Taq DNA Polymerase (Invitrogen) and SYBR Green quantification, according to the manufacturer's instructions. Results for Mrp2 and Bsep mRNA were normalized to the expression of 18S rRNA as the housekeeping gene, by using the $2^{-\Delta\Delta Ct}$ method [33].

Table 1. Sequence of primers used in Real-time PCR.

Gen target	Primer	Primer sequence (5' → 3')
Bsep	Forward	CCGAAGGCTCAGGGTATTGG
	Reverse	ATCAGGTGACATGGTGGCAG
Mrp2	Forward	ACCTTCCACGTAGTGATCCT
	Reverse	ACCTGCTAAGATGGACGGTC
18s rRNA	Forward	GTAACCCGTTGAACCCCATT
	Reverse	CCATCCAATCGGTAGTAGCG

2.9. Immunofluorescence detection of Bsep and Mrp2

Liver pieces were immersed in isopentane at -70 °C, immediately removed, and stored at -70 °C until use. The tissues were then cut into 5 µm slices with a cryostat, fixed and stained, as described previously [34]. For immunolabeling, tissue sections were incubated overnight with a rabbit anti-rat Bsep (1:200; Kamiya Biomedical Co., Seattle, WA, USA), or with a mouse anti-rat Mrp2 (1:200; [M2III-6]; Alexis Biochemicals, San Diego, CA, USA), followed by incubation with a Cy2-conjugated donkey anti-rabbit IgG or a Cy2-conjugated donkey anti-mouse IgG, respectively (1:200, 1 h; Jackson ImmunoResearch Laboratory, West Grove, PA). To delimitate the bile canaliculi, the tight junctional-associated protein occludin was used. Occludin was labeled with a mouse anti-rat occludin (when Bsep immunostaining was carried out, 1:200, overnight;

Invitrogen) or with a rabbit anti-rat occludin (when Mrp2 immunostaining was carried out, 1:200, overnight; Zymed, San Francisco, USA), followed by incubation with a Cy3-conjugated donkey anti-mouse or a Cy3-conjugated donkey anti-rabbit (1:200, 1 h, Jackson ImmunoResearch Laboratory, West Grove, PA.), respectively. The images were captured on a LSM880, Carl Zeiss LLC (Thornwood, NY, USA) confocal microscope. To ensure comparable staining and image capture performance for all groups, liver slices were prepared on the same day, mounted on the same glass slide, and subjected to the staining process and microscopy analysis simultaneously. Quantification of the degree of Bsep and Mrp2 endocytic internalization was performed on confocal images using ImageJ 1.34 m (National Institutes of Health), as described by us elsewhere [35]. For this purpose, fluorescence intensity associated with the transporters along an 8 μm line perpendicular to the canaliculus (from −4 μm to 4 μm of the canalicular center) was assessed. For each section, data from at least 10 different canaliculi were collected, and used for statistical comparison.

2.10. Statistical analysis

Data are expressed as means ± SEM. Statistical analysis was carried out by using ANOVA or Student *t* test, unless another statistical test has been determined to be more appropriate. The variances of the densitometric profiles of Bsep and Mrp2 localization were compared with the Mann-Whitney U test [36]. Values of $P < 0.05$ were considered to be statistically significant.

3. Results

3.1. Biliary and plasma parameters of cholestasis

A significant decrease in BF was observed in LPS group while, in the co-treated group, BF was restored to control values (Table 2). At the same time, there was a tendency to increase BF in SL-treated animals. A decrease in TBA output and in total GSH output was observed in the LPS group. In the SL+LPS group, TBA output remained unchanged as compared to the LPS group. However, total GSH output was significantly increased in the co-treated group, as compared to the LPS group. There was a tendency to increase in total GSH output in the SL group compared with control group. These changes in GSH excretion were in agreement with the changes observed in BSIBF. This parameter accounted for 83% of total basal bile flow, a relative contribution in line with previous results from us [15,37] and others [38,39], and was reduced by 37% in LPS-treated rats. SL had a tendency towards increasing BSIBF when administered alone, and normalized this parameter in LPS-co-treated animals (Table 2).

Table 2. Basal biliary parameters.

	Control	SL	LPS	SL+LPS
BF (µl/min per g liver)	3.5 ± 0.1	3.9 ± 0.2	2.4 ± 0.1*	3.1 ± 0.2$^{\#}$
TBA output (nmol/min per g liver)	52 ± 8	43 ± 7	31 ± 3*	30 ± 4*
Total GSH output (nmol/min per g liver)	1.35 ± 0.11	1.71 ± 0.24	0.37 ± 0.05*	0.76 ± 0.12*$^{\#}$
BSIBF (µl/min per g liver)	3.0 ± 0.2	3.6 ± 0.2	1.9 ± 0.1*	2.8 ± 0.1$^{\#}$

BF, bile flow; BSIBF; bile salt independent bile flow; GSH, glutathione; LPS, lipopolysaccharide; SL, spironolactone; TBA, total bile acids.

*P < 0.05 *vs.* control; $^{\#}$P < 0.05 *vs.* LPS. *n* = 3-15.

Regarding plasma biochemical parameters, ALP was increased in the LPS group and this was not prevented by the SL pre-treatment (Table 3). On the other hand, there were no changes in plasma levels of AST, ALT, and LDH in LPS-treated animals compared with control group, irrespective of whether they have been co-treated with SL or not.

Table 3. Plasma biochemical parameters.

	Control	SL	LPS	SL+LPS
ALP (U/l)	370 ± 24	402 ± 43	535 ± 56*	516 ± 68*
AST (U/l)	135 ± 16	113 ± 11	145 ± 27	168 ± 23
ALT (U/l)	42 ± 16	35 ± 7	41 ± 16	28 ± 7
LDH (U/l)	381 ± 29	364 ± 24	559 ± 119	640 ± 197

ALP, alkaline phosphatase; AST, aspartate aminotransferase; ALT, alanine aminotransferase; LDH, lactate dehydrogenase; LPS, lipopolysaccharide; SL, spironolactone; TBA, total bile acids.

*P < 0.05 *vs.* control; #P < 0.05 *vs.* LPS. *n* = 4-13.

3.2. Biliary excretion of exogenous Mrp2 and Bsep substrates

Mrp2 transport activity was estimated following a bolus injection of DBSP, a model Mrp2 substrate. As depicted in Fig. 1, DBSP was transported less efficiently by LPS-treated rats. This impairment was however partially counteracted by SL pre-treatment, since cumulative biliary excretion of DBSP in the co-treated rats was intermediate between LPS and control groups. This is consistent with the our previous results here for the total

output of GSH, a Mrp2 substrate, further supporting the fact that SL pre-treatment prevented the Mrp2 secretory failure induced by LPS.

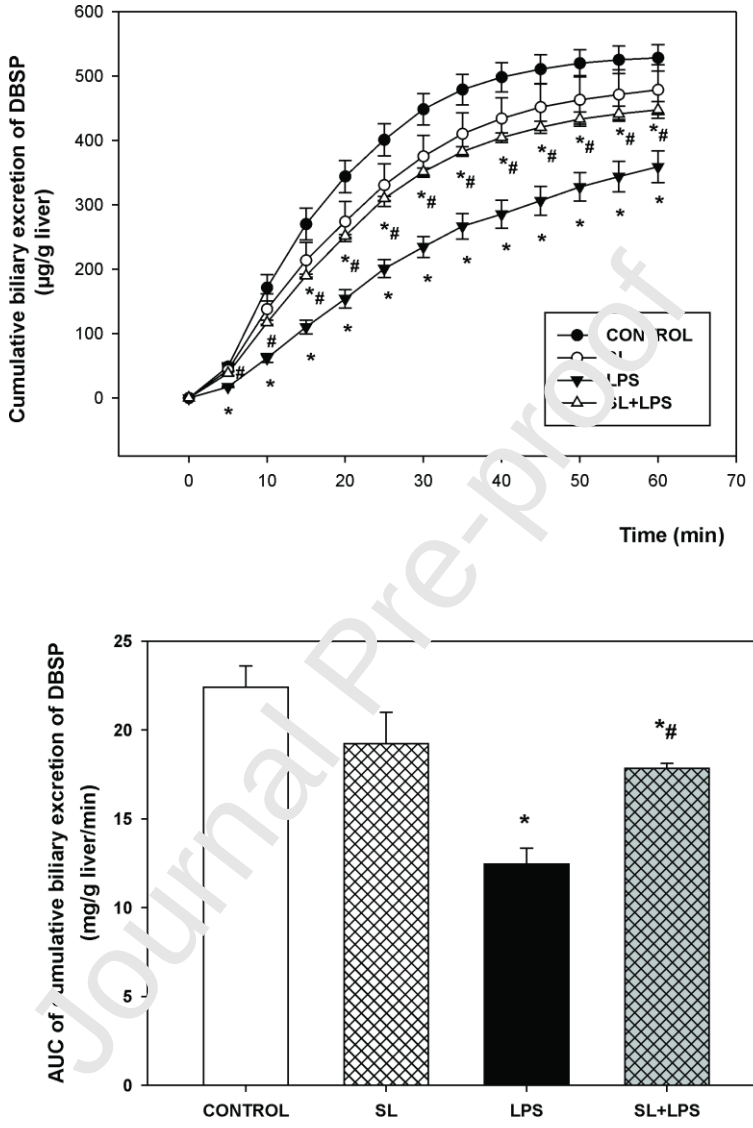

Figure 1. ***Upper panel.*** **Cumulative biliary excretion of dibromosulfophthalein (DBSP)**. Bile samples were collected every 5 min for 60 min, after a single, i.v. dose of 15 mg/kg of b.w. ***Lower panel.*** **Area under the curve (AUC) of cumulative biliary excretion of DBSP**. LPS, lipopolysaccharide; SL, spironolactone. Data are mean ±

SEM, for 3-5 individual experiments. Data are shown as mean ± SEM. *P < 0.05 *vs.* control; #P < 0.05 *vs.* LPS.

Bsep transport function was estimated by recording changes over time in biliary excretion of TC, following a bolus injection of this compound. Then, BF and TBA output over basal values, attributed to the output of exogenously administered TC, were analyzed (Table 4, Fig. 2). A decrease in these parameters was found in the LPS group. In the SL+LPS group, TBA output values remains similar to those in the LPS group. SL had per se an inhibitory effects on TC biliary excretion, but the difference was only apparent during the first two time periods of bile collection after TC injection.

Table 4. TC-stimulated biliary parameters.

	Control	SL	LPS	SL+LPS
TC-stimulated† BF (µl/min per g liver)	5.8 ± 0.1	5.5 ± 0.1	3.4 ± 0.1*	4.3 ± 0.1*#
TC-stimulated† TBA output (nmol/min per g liver)	237 ± 17	212 ± 37	129 ± 9*	151 ± 3*

BF, bile flow; LPS, lipopolysaccharide; SL, spironolactone; TC, taurocholate; TBA, total bile acids.

†TC-stimulated values correspond to the maximum value obtained after a TC i.v. injection of 8 µmol/100 g of b.w.

*P < 0.05 *vs.* control; #P < 0.05 *vs.* LPS. *n* = 3-4.

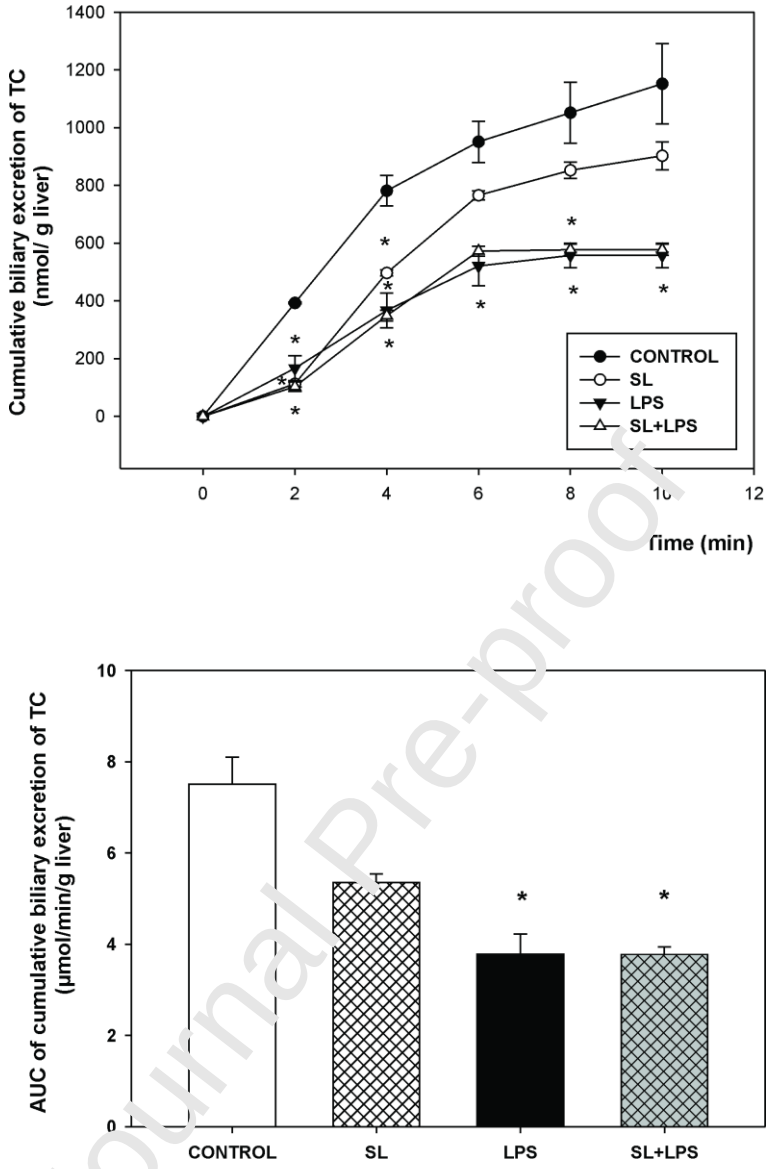

Figure 2. ***Upper panel.*** **Cumulative biliary excretion of taurocholate (TC)**. Bile samples were collected every 2 min for 10 min, after a single, i.v. dose of 8 µmol/100 g of b.w. of the BS. ***Lower panel.*** **Area under the curve (AUC) of cumulative biliary excretion of TC.** LPS, lipopolysaccharide; SL, spironolactone. Data are mean ± SEM, for 3 individual experiments. Data are shown as mean ± SEM. *P < 0.05 *vs.* control; $^{\#}$P < 0.05 *vs.* LPS.

3.3. Mrp2 and Bsep mRNA expression

In LPS-treated animals, a decrease in both Mrp2 and Bsep, was observed. In SL+LPS co-treated animals, an increase in Mrp2, but not in Bsep mRNA expression was found (Table 5). An increase in Mrp2 mRNA expression in SL group was also recorded.

Table 5. Mrp2 and Bsep mRNA expression by Real-time PCR.

mRNA levels (% of mean control values)	Control	SL	LPS	SL+LPS
Mrp2	100 ± 6	145 ± 2*	64 ± 5*	85 ± 6#
Bsep	100 ± 12	82 ± 11	39 ± 3*	36 ± 2*

LPS, lipopolysaccharide; SL, spironolactone.

*P < 0.05 vs. control; #P < 0.05 vs. LPS. n = 3-7.

3.4. Western blot analysis of Mrp2 and Bsep expression

Mrp2 protein expression was significantly reduced, both at plasma membrane and total homogenate levels, in the LPS-treated group (Fig. 3). An increase in SL+LPS co-treated animals was observed in both fractions. In SL control group, Mrp2 protein expression increase in total homogenate and plasma membrane. This is in agreement with the

increase in mRNA levels of Mrp2, and with previous reports on induction of Mrp2 by SL [15,16].

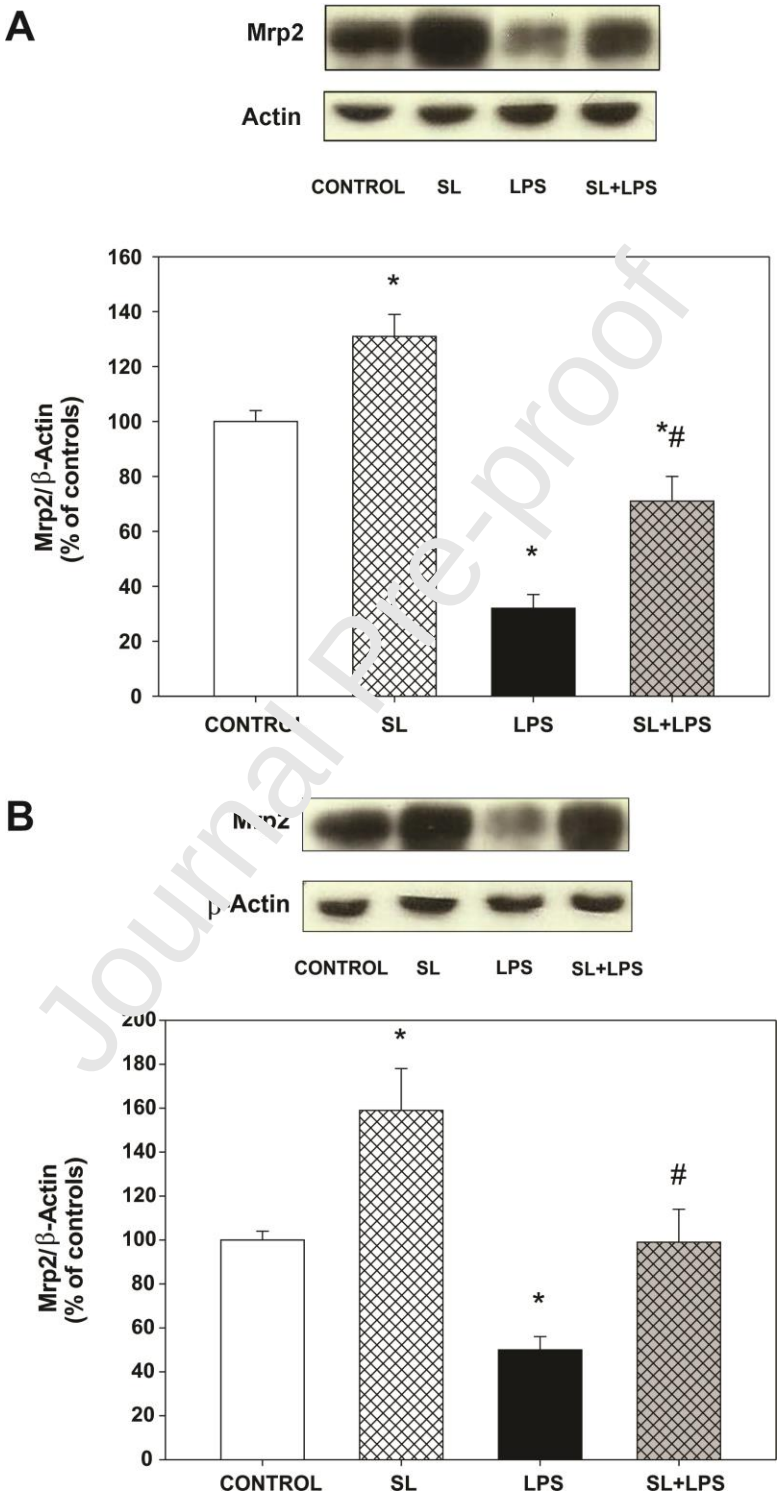

Figure 3. Protein expression of Mrp2. *A*. Western blot analysis of Mrp2 in liver homogenate. *B*. Western blot analysis of Mrp2 in liver plasma membranes. Data on densitometric analysis are presented as percentages and were referred to control, considered as 100%. Differences in sample loading were corrected by the densitometric signal of the corresponding actin band. LPS, lipopolysaccharide; SL, spironolactone. Data are shown as mean ± SEM. *P < 0.05 *vs.* control; $^{\#}$P < 0.05 *vs.* LPS. *n* = 8-10.

A decrease in Bsep protein expression was also found in liver plasma membranes and homogenate in the LPS-treated group (Fig. 4). In SL+LPS co-treated animals, an increase in Bsep protein expression at the plasma membrane level was observed, but not in liver homogenate. Although, there was a tendency towards increased Bsep protein levels in homogenate when compared to the LPS group, the difference did not reach statistical significance.

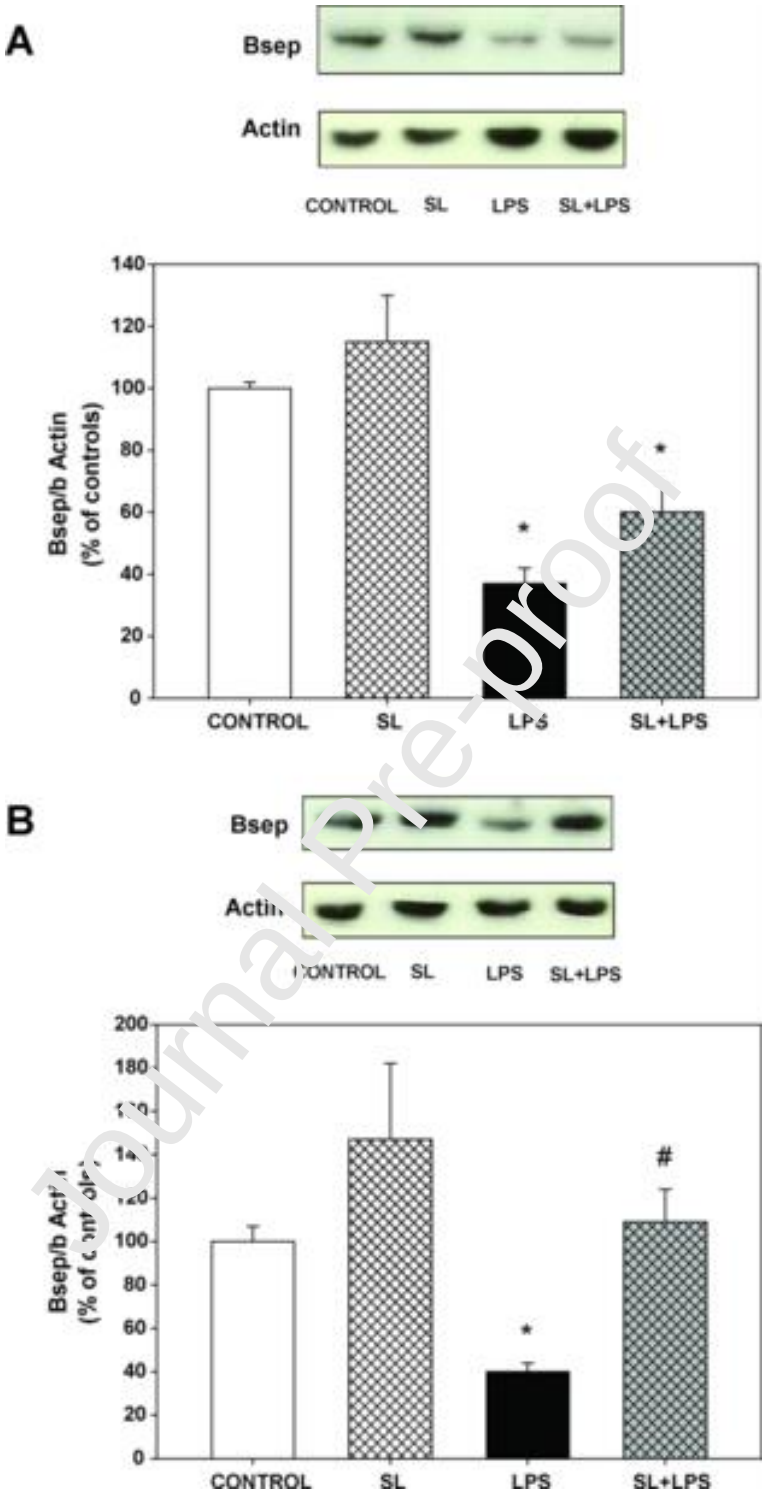

Figure 4. Protein expression of Bsep. A. Western blot analysis of Bsep in liver homogenate. B. Western blot analysis of Bsep in liver plasma membranes. Data

on densitometric analysis are presented as percentages and were referred to control considered as 100%. Differences in sample loading were corrected by the densitometric signal of the corresponding actin band. LPS, lipopolysaccharide; SL, spironolactone. Data are shown as mean ± SEM. *P < 0.05 *vs.* control; $^{\#}$P < 0.05 *vs.* LPS. *n* = 6-10.

Due to the increase in the protein expression levels of both transporters in liver membranes, a possible post-translational regulation associated with an improvement in plasma membrane localization was suggested. Therefore, we studied their localization status by confocal microscopy.

3.5. Mrp2 and Bsep localization by immunofluorescence followed by confocal microscopy

Fig. 5A shows confocal images of Mrp2 (stained in green) and occludin, used as a marker of the bile canaliculus edge (stained in red). The transporter was localized in the canalicular membrane in liver slices of control and SL-treated animals, while in livers of the LPS group, a re-localization of Mrp2 outside the limits of the canaliculus was observed. Pretreatment with SL prevented this internalization of Mrp2 from the canalicular membrane to pericanalicular endosomes. Fig. 5B shows the distribution profiles of transporter-associated fluorescence along a line perpendicular to the bile canaliculus. Analysis of the distribution profiles of occludin demonstrates a conserved width of the canaliculi in all groups, thus ruling out changes in the canaliculi structure

that could have affected localization of Bsep. The same results were observed for Bsep localization analysis (Fig. 6).

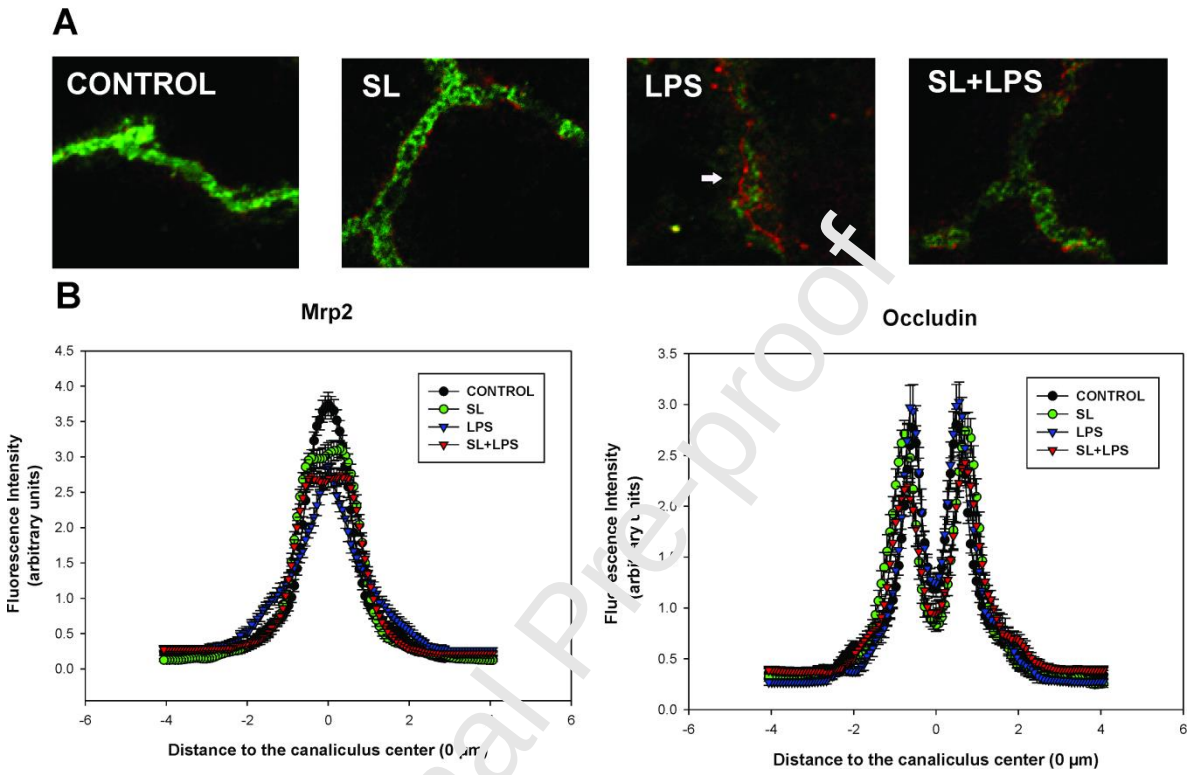

Figure 5. Endocytic internalization of Mrp2. ***A.*** Representative confocal images showing co-immunostaining of Mrp2 (green) and occludin (red; marker of the bile canaliculus edge), illustrative of the endocytic internalization of Mrp2 induced by lipopolysaccharide (LPS; arrows), and its prevention by spironolactone (SL). ***B.*** Lower panels show densitometric analysis of the fluorescence intensity associated with Mrp2 or occluding, along an 8-µm line perpendicular to the bile canaliculus (from −4 µm to +4 µm from the canalicular centre), corresponding to the confocal images shown in the upper panels. Data are shown as mean ± SEM, for at least 10 different canaliculi.

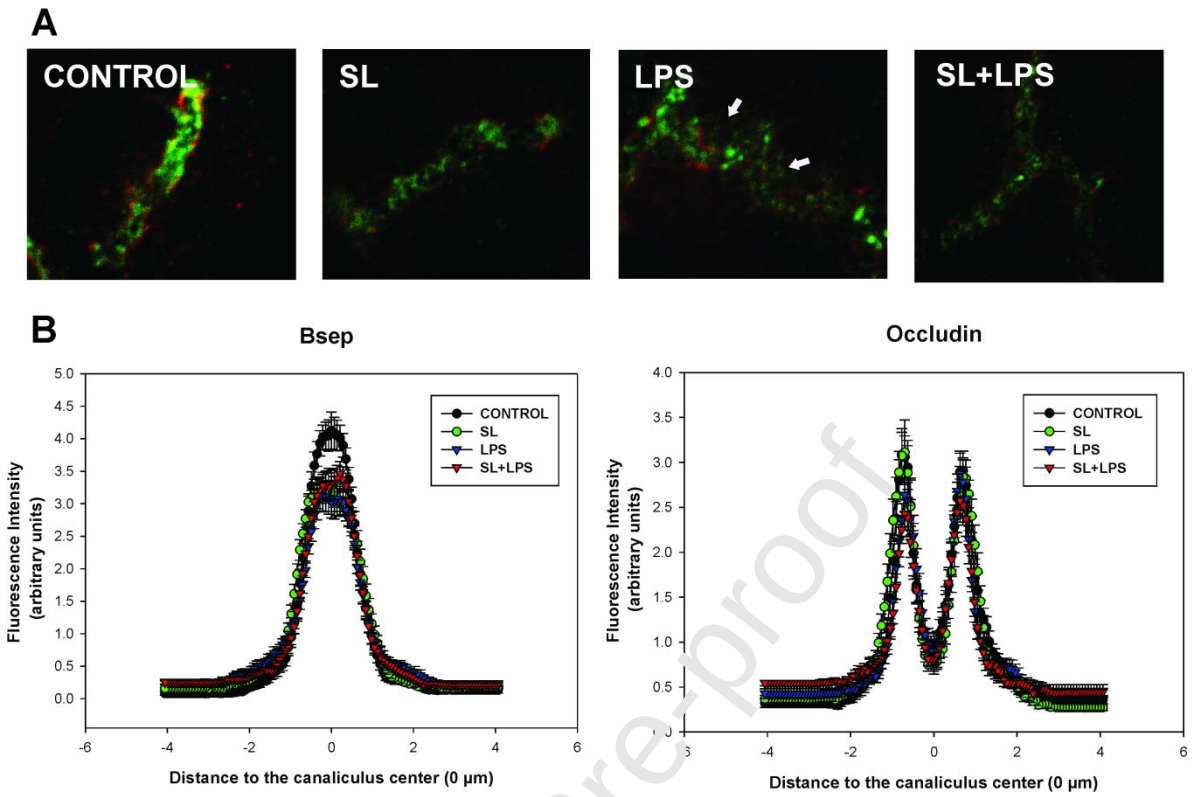

Figure 6. Endocytic internalization of Bsep. ***A.*** Representative confocal images showing co-immunostaining of Bsep (green) and occludin (red; marker of the bile canaliculus edge), illustrative of the endocytic internalization of Bsep induced by lipopolysaccharide (LPS; arrows), and its partial prevention by spironolactone (SL). ***B.*** Lower panels show densitometric analysis of the fluorescence intensity associated with Bsep or occludin along an 8-µm line perpendicular to the bile canaliculus (from −4 µm to +4 µm from the canalicular centre), corresponding to the confocal images shown in the upper panels. Data are shown as mean ± SEM, for at least 10 different canaliculi.

3.6. Pro-inflammatory cytokines

IL-1β, TNF-α and IL-6 were increase in LPS-treated animals, 2 hours after the second dose of LPS. However, SL pre-treatment did not prevent these effects (Table 6). We therefore inferred that the beneficial effects of SL did not involve inhibition of the inflammatory response.

Table 6. Plasma levels of pro-inflammatory cytokines, IL-1β, TNF-α and IL-6.

Pro-inflammatory cytokines	Control	SL	LPS	SL+LPS
IL-1β (pg/mL)	190 ± 44	198 ± 45	648 ± 78*	517 ± 61*
TNF-α (pg/mL)	13 ± 1	8 ± 1	30 ± 9	17 ± 1*
IL6 (pg/mL)	108 ± 24	129 ± 35	2130 ± 222*	1685 ± 101*

IL-1β, interleukin-1β; IL-6, interleukin-6; LPS, lipopolysaccharide; SL, spironolactone TNF-α, tumor necrosis factor-α.

*P < 0.05 vs. control; #P < 0.05 vs. LPS. n = 3-4.

4. Discussion

In this study, we showed that SL was instrumental in preventing some relevant cholestatic effects of LPS. It extensively improved the BSIBF, a phenomenon involving restoration of the biliary excretion of GSH, the main solute responsible for its generation [40], via a functional improvement of its canalicular transporter Mrp2, through both transcriptional and post-transcriptional mechanisms.

In a previous work [10], we analyzed the anti-cholestatic effects of UDCA, the first-choice therapy for most cholestatic diseases, in LPS-induced cholestasis. We found that UDCA has only partial effects on the restoration of the biliary secretory function, which are complementary to the anti-cholestatic mechanisms shown to be afforded here by SL. Indeed, UDCA was unable to improve BSIBF, as a consequence of its inability to prevent the functional failure and protein expression impairment of Mrp2 induced by LPS. Therefore, in an attempt to restore Mrp2 functionality, we assayed an alternative anti-cholestatic strategy based on the transactivation of PXR, the main nuclear receptor responsible for regulating Mrp2 expression [41], by using SL, a recognized PXR ligand able to improve Mrp2 expression at a transcriptional level [15].

Although, in humans, one of the most potent PXR ligands is rifampicin [42], it is a weak ligand in rodents, so that we decided to use SL, as an alternative ligand with far higher affinity for rat PXR [12,13].

BF restoration was observed towards control levels in co-treated animals (see Table 2). This effect was attributed to an improvement in BSIBF, associated with an increase in

total GSH output in co-treated animals compared to LPS group (see Table 2). GSH is excreted towards the lumen of the bile canaliculus via Mpr2 [43], so that an increase in its excretion could indicate an improvement in transporter functionality. To become independent of possible variations in intracellular GSH levels, we studied Mrp2 functionality by using the exogenous substrate of the transporter, DBSP. We recorded an improvement in DBSP excretion in co-treated animals (see Fig. 1), thus confirming an increase in Mrp2 functionality in SL+LPS co-treated animals. When evaluating Mrp2 mRNA levels, we observed an increase in co-treated animals compared to the LPS group (see Table 5), which was correlated with increased protein levels, both in plasma membrane fraction and in total homogenate (see Fig. 3). This is most likely related to the transactivating effect of SL on PXR, since, PXR positively modulates Mrp2 expression [14,15]. Regardless of the mechanisms involved, the complete restoration of Mrp2 activity in LPS-treated rats could have important clinical implications, not only by ameliorating the cholestasis itself but also by counteracting the hyperbilirubinemia that occurs in sepsis-induced cholestasis [1]. Indeed, Mrp2 is the limiting step for bilirubin metabolite excretion into bile [44], and its improvement should certainly result in an improved biliary clearance of this potentially toxic compound. Unfortunately, the rat has a very high reserve capacity to clear bilirubin, with $t_{1/2}$ being 26 times faster than in humans [45], and therefore its levels were not increased in plasma in our model (data not shown), thus preventing us from ascertaining whether SL is actually effective in reducing bilirubin levels in an hyperbilirubinemic condition associated with endotoxemia.

Regarding Bsep, mRNA levels in the SL+LPS co-treated group remained lower than control levels, and similarly low to those in the LPS group (see Table 5). This was

reflected in low Bsep protein expression levels in total homogenate in the co-treated group (see Fig. 4), and low biliary excretion of BS, both under basal and TC-stimulated conditions (see Tables 2 and 4, and Fig. 2). This finding is consistent with the high ALP plasma levels observed in the co-treated animals (see Table 3). We inferred that hepatocytes would not be able to counteract BS overload through the Bsep canalicular transporter, and this would generate a removal of protein components from the plasma membrane due to its surfactant effect, thus releasing ALP to plasma. These results are consistent with previous studies where there were no changes in Bsep expression in rats treated with SL alone [15], or in the expression of the BS export pump Mrp3 involved in basolateral BS efflux either in normal rats or in rats with ethynylestradiol-induced cholestasis [16].

An increase in Bsep protein levels was found in the plasma membrane fraction (although not in total homogenate) (see Fig. 4), which would indicate some kind of post-translational regulation, for example, increased transporter stability in the canalicular membrane against the endocytic stimulation induced by LPS [9]. This beneficial effect of SL was also extended to Mrp2, since it was also better localized in plasma membrane in the co-treated group. To test this hypothesis, we studied the subcellular localization of Mrp2 and Bsep by confocal microscopy, and we confirmed that both Mrp2 and Bsep are better located in the canaliculi in co-treated animals, but not in the LPS group, where the transporter is internalized in intracellular vesicular compartments (see Figs. 5 and 6); this contributes to explain the recovery in the expression of both transporters in the plasma membrane fraction. This post-translational effect of SL was somewhat unexpected for a compound presumed to exert its effects primarily by transcriptional

mechanisms. However, some properties of SL on liver structure and function provide some hints. SL decreases plasma membrane fluidity, as a result of an increase in cholesterol and a decrease in phospholipids [46]. On the other hand, LPS treatment decreases cholesterol content in the canalicular membrane [47], an effect that could have been counteracted by SL co-treatment. SL effect would enable the stabilization of the transporters in lipid raft microdomains, thus preventing their transfer to non-raft structures, and their further endocytosis via a clathrin-dependent mechanism [48]. Another possibility could involve certain antioxidant effects exerted by SL. Internalization of transporters in LPS-induced cholestasis, but not the transporter downregulation at transcriptional level, has been causally associated with the induction of oxidative stress caused by endotoxin, since antioxidant agents completely prevented this effect [49]. Suggestively, SL showed antioxidant effects in a wide variety of tissues and, particularly, in the liver, where it was able to inhibit pro-oxidant systems (e.g., NADPH oxidase) [50] and induce antioxidant systems (e.g., catalase) [51]. Undoubtedly, this and other effects of SL not related to PXR deserve to be studied in more detail to fully understand its post-transcriptional anti-cholestatic action mechanisms.

The improvement in Bsep localization in plasma membrane in SL+LPS co-treated animals compared to LPS-treated group did not have the expected impact on its transporter activity (see Table 4 and Fig. 2). This result would indicate that, although Bsep is correctly localized, its intrinsic transport activity is selectively inhibited. Although an increase in membrane cholesterol could be beneficial because it improves its localization in lipid raft microdomains, excessive cholesterol content decreases

canalicular membrane fluidity [52], a factor thought to influence Bsep transport activity [53,54]; this may explain the somewhat lower Bsep-mediated transport of the exogenously administered TC in the SL alone group (see Fig. 2). The 'rigidizing' effect of SL could be particularly detrimental in endotoxemic rats, since LPS per se reduces hepatocellular membrane fluidity by increasing the cellular influx of Ca^{2+} [55], an effect that would add to the 'rigidizing' effect of SL itself, which may further decrease plasma membrane fluidity by alternative mechanisms associated with its effect as an aldosterone antagonist or as an estrogen-mimetic compound [46]. Unlike Bsep, circumstantial evidence suggest that Mrp2 transport function is scantily influenced by diminutions of plasma membrane fluidity [54], thus explaining the lack of impairment in DBSP biliary excretion when SL was administered alone (see Fig. 1), and the good relationship between improved localization and enhanced function observed for Mrp2 in SL+LPS co-treated group (see Figs. 1 and 5), as opposed to Bsep.

Finally, we evaluated the potential anti-inflammatory role of SL as PXR ligand in LPS-induced cholestasis, because this effect of PXR had been shown in other inflammatory models [17,18]. For this purpose, we determine a series of pro-inflammatory cytokines in plasma (see Table 6). We do not observe changes in their plasma levels in the SL+LPS group compared to the LPS group, thus ruling out the possibility that the SL acts in this model via inhibition of NF-κB [18], the main transcription factor mediating LPS-induced inflammatory response. Although, anti-inflammatory effects of SL had been previously described, they are not related to its properties as PXR activator, but to the antagonistic effect on aldosterone, an ubiquitous hormone that exerts pro-inflammatory effects [56], but not related to endotoxemia.

5. Conclusion

Our results show that the PXR ligand SL contributes to normalize BF in LPS-induced cholestasis by improving Mrp2 expression and localization, thus allowing the recovery of mechanisms of bile formation independent of BS excretion. This properly complements others experimental anti-cholestatic approaches that, like that involving UDCA administration, failed to improve these mechanisms of BF generation while improving others related to BS excretion. This allows to envisage the need for complementary co-treatments to successfully treat this complex condition, with PXR ligands been key parts of these therapeutic options.

Conflict of interest

The authors have no conflict of interest.

Acknowledgement

We thank Rodrigo Vena for their valuable technical assistance in confocal imaging.

Funding information

This work was supported by grants from Agencia Nacional de Promoción Científica y Tecnológica, Argentina (PICT-2013-0974 and PICT-2016-1613) and Consejo Nacional de Investigaciones Científicas y Técnicas (PIP 112-201201-00217 and PUE-0089).

References

[1] H.K. Bhogal, A.J. Sanyal, The molecular pathogenesis of cholestasis in sepsis, Front. Biosci. (Elit. Ed.) 5 (2013) 87–96. https://doi.org/10.2741/e598.

[2] M. Trauner, P. Fickert, R.E. Stauber, Inflammation-induced cholestasis, J. Gastroenterol. Hepatol. 14 (1999) 946–959. https://doi.org/10.1046/j.1440-1746.1999.01982.x.

[3] R.K. Gilroy, M.E. Mailliard, J.L. Gollan, Cholestasis of sepsis, Bailliere's Best Pract. Res. Clin. Gastroenterol. 17 (2003) 357–367. https://doi.org/10.1016/S1521-6918(03)00027-1.

[4] S. Dizier, J.M. Forel, L. Ayzac, C. Richard, S. Hraiech, S. Lehingue, A. Loundou, A. Roch, C. Guerin, L. Papazian, Early hepatic dysfunction is associated with a worse outcome in patients presenting with acute respiratory distress syndrome: A post-hoc analysis of the ACURASYS and PROSEVA studies, PLoS One 10 (2015) e0144278. https://doi.org/10.1371/journal.pone.0144278.

[5] N.J. Cherrington, A.L. Slitt, N. Li, C.D. Klaassen, Lipopolysaccharide-mediated regulation of hepatic transporter mRNA levels in rats, Drug Metab. Dispos. 32 (2004) 734–741. https://doi.org/10.1124/dmd.32.7.734.

[6] T.A. Vos, G.J.E.J. Hooiveld, H. Koning, S. Childs, D.K.F. Meijer, H. Moshage, P.L.M. Jansen, M. Müller, Up-regulation of the multidrug resistance genes, Mrp1 and Mdr1b, and down-regulation of the organic anion transporter, Mrp2, and the bile salt transporter, Spgp, in endotoxemic rat liver, Hepatology 28 (1998) 1637–1644.

https://doi.org/10.1002/hep.510280625.

[7] Z.C. Gatmaitan, A.T. Nies, I.M. Arias, Regulation and translocation of ATP-dependent apical membrane proteins in rat liver, Am. J. Physiol. (Gastrointest. Liver Physiol.) 272 (1997) G1041-G1049. https://doi.org/10.1152/ajpgi.1997.272.5.g1041.

[8] A. Geier, M. Wagner, C.G. Dietrich, M. Trauner, Principles of hepatic organic anion transporter regulation during cholestasis, inflammation and liver regeneration, Biochim. Biophys. Acta (Mol. Cell Res.) 1773 (2007) 283–308. https://doi.org/10.1016/j.bbamcr.2006.04.014.

[9] M.G. Roma, I.M. Barosso, G.S. Miszczuk, F.A. Crocenzi, E.J. Sanchez Pozzi, Dynamic localization of hepatocellular transporters: role in biliary excretion and impairment in cholestasis, Curr. Med. Chem. 26 (2019) 1113–1154. https://doi.org/10.2174/0929867325666171205153204.

[10] M.V. Razori, P.M. Maidagan, N. Ciriaci, R.B. Andermatten, I.R. Barosso, P.L. Martín, C.L. Basiglio, E.J. Sánchez Pozzi, M.L. Ruiz, M.G. Roma, Anticholestatic mechanisms of ursodeoxycholic acid in lipopolysaccharide-induced cholestasis, Biochem. Pharmacol. 168 (2019) 48–56. https://doi.org/10.1016/j.bcp.2019.06.009.

[11] H.R. Ochs, D.J. Greenblatt, S. Bodem, T.W. Smith, Spironolactone, Am. Heart J. 96 (1978) 389–400. https://doi.org/10.1016/0002-8703(78)90052-2.

[12] E.G. Schuetz, C. Brimer, J.D. Schuetz, Environmental xenobiotics and the antihormones cyproterone acetate and spironolactone use the nuclear hormone pregnenolone X receptor to activate the CYP3A23 hormone response element, Mol.

Pharmacol. 54 (1998) 1113–1117. https://doi.org/10.1124/mol.54.6.1113.

[13] S.A. Kliewer, B. Goodwin, T.M. Willson, The nuclear pregnane X receptor: A key regulator of xenobiotic metabolism, Endocr. Rev. 23 (2002) 687–702. https://doi.org/10.1210/er.2001-0038.

[14] S. Kakizaki, D. Takizawa, H. Tojima, N. Horiguchi, Y. Yamazaki, M. Mori, Nuclear receptors CAR and PXR; Therapeutic targets for cholestatic liver disease, Front. Biosci. 16 (2011) 2988–3003. https://doi.org/10.2741/3893.

[15] M.L. Ruiz, S.S. Silvina, M.G. Luquita, E.J. Sánchez-Pozzi, F.A. Crocenzi, J.M. Pellegrino, J.E. Ochoa, M. Vore, A.D. Mottino, V.A. Catania, Mechanisms involved in spironolactone-induced choleresis in the rat. Role of multidrug resistance-associated protein 2, Biochem. Pharmacol. 69 (2005) 531–539. https://doi.org/10.1016/j.bcp.2004.10.017.

[16] M.L. Ruiz, S.S.M. Villanueva, M.G. Luquita, S.I. Ikushiro, A.D. Mottino, V.A. Catania, Beneficial effect of spironolactone administration on ethynylestradiol- induced cholestasis in the rat: Involvement of up-regulation of multidrug resistance-associated protein 2, Drug Metab. Dispos. 35 (2007) 2060–2066. https://doi.org/10.1124/dmd.107.016519.

[17] M. Sun, W. Cui, S.K. Woody, J.L. Staudinger, Pregnane X receptor modulates the inflammatory response in primary cultures of hepatocytes, Drug Metab. Dispos. 43 (2015) 335–343. https://doi.org/10.1124/dmd.114.062307.

[18] C. Zhou, M.M. Tabb, E.L. Nelson, F. Grün, S. Verma, A. Sadatrafiei, M. Lin, S.

Mallick, B.M. Forman, K.E. Thummel, B. Blumberg, Mutual repression between steroid and xenobiotic receptor and NF-κB signaling pathways links xenobiotic metabolism and inflammation, J. Clin. Invest. 116 (2006) 2280–2289. https://doi.org/10.1172/JCI26283.

[19] A. Esteller, Physiology of bile secretion, World J. Gastroenterol. 14 (2008) 5641–5649. https://doi.org/10.3748/wjg.14.5641.

[20] F. Tietze, Enzymic method for quantitative determination of nanogram amounts of total and oxidized glutathione: Applications to mammalian blood and other tissues, Anal. Biochem. 27 (1969) 502–522. https://doi.org/10.1016/0003-2697(69)90064-5.

[21] O.W. Griffith, Determination of glutathione and glutathione disulfide using glutathione reductase and 2-vinylpyridine, Anal. Biochem. 106 (1980) 207–212. https://doi.org/10.1016/0003-2697(80)90139-6.

[22] D.R. Johnson, C.D. Klaassen, Role of rat multidrug resistance protein 2 in plasma and biliary disposition of dibromosulfophthalein after microsomal enzyme induction, Toxicol. Appl. Pharmacol. 180 (2002) 56-63. https://doi.org/10.1006/taap.2002.9375.

[23] A. Geier, C.G. Dietrich, S. Voigt, S.-K. Kim, T. Gerloff, G.A. Kullak-Ublick, J. Lorenzen, S. Matern, C. Gartung, Effects of proinflammatory cytokines on rat organic anion transporters during toxic liver injury and cholestasis, Hepatology 38 (2003) 345–354. https://doi.org/10.1053/jhep.2003.50317.

[24] H. Kouzuki, H. Suzuki, K. Ito, R. Ohashi, Y. Sugiyama, Contribution of sodium taurocholate co-transporting polypeptide to the uptake of its possible substrates into rat hepatocytes, J. Pharmacol. Exp. Ther. 286 (1998) 1043–1050, doi: not available.

[25] M. Müller, T. Ishikawa, U. Berger, C. Klünemann, L. Lucka, A. Schreyer, C. Kannicht, W. Reutter, G. Kurz, D. Keppler, ATP-dependent transport of taurocholate across the hepatocyte canalicular membrane mediated by a 110-kDa glycoprotein binding ATP and bile salt, J. Biol. Chem. 266 (1991) 18920–18926, doi: not available.

[26] U. Bolder, H.T. Ton-Nu, C.D. Schteingart, E. Frick, A.F. Hofmann, Hepatocyte Transport of bile acids and organic anions in endotoxemic rats: impaired uptake and secretion, Gastroenterology 112 (1997) 214–225. https://doi.org/10.1016/s0016-5085(97)70238-5.

[27] T. Gerloff, B. Stieger, B. Hagenbuch, J. Madon, L. Landmann, J. Roth, A.F. Hofmann, P.J. Meier, The sister of P-glycoprotein represents the canalicular bile salt export pump of mammalian liver, J. Biol. Chem. 273 (1998) 10046–10050. https://doi.org/10.1074/jbc.273.16.10046.

[28] N.B. Javitt, Phenol 3, 6 dibromphthalein disulfonate, a new compound for the study of liver disease, Proc. Soc. Exp. Biol. Med. 117 (1964) 254–257. https://doi.org/10.3181/00379727-117-29550.

[29] V.A. Catania, M.G. Luquita, E.J. Sánchez Pozzi, A.D. Mottino, Differential induction of glutathione S-transferase subunits by spironolactone in rat liver, jejunum and colon, Life Sci. 63 (1998) 2285–2293. https://doi.org/10.1016/S0024-

3205(98)00517-7.

[30] P.L.M. Jansen, G.M.M. Groothuis, W.H.M. Peters, D.F.M. Meijer, Selective hepatobiliary transport defect for organic anions and neutral steroids in mutant rats with hereditary-conjugated hyperbilirubinemia, Hepatology 7 (1987) 71–76. https://doi.org/10.1002/hep.1840070116.

[31] J.L. Boyer, Bile formation and secretion, Compr. Physiol. 3 (2013) 1035–1078. https://doi.org/10.1002/cphy.c120027.

[32] R. Kubitz, A. Helmer, D. Häussinger, Biliary transport systems: Short-term regulation, Methods Enzymol. 400 (2005) 542–557. https://doi.org/10.1016/S0076-6879(05)00030-3.

[33] M.W. Pfaffl, A new mathematical model for relative quantification in real-time RT-PCR, Nucleic Acids Res. 29 (2001) 45e. https://doi.org/10.1093/nar/29.9.e45.

[34] A.D. Mottino, J. Cao, L.M. Veggi, F. Crocenzi, M.G. Roma, M. Vore, Altered localization and activity of canalicular Mrp2 in estradiol-17β-D-glucuronide-induced cholestasis, Hepatology 35 (2002) 1409–1419. https://doi.org/10.1053/jhep.2002.33327.

[35] F.A. Crocenzi, A.D. Mottino, J. Cao, L.M. Veggi, E.J.S. Pozzi, M. Vore, R. Coleman, M.G. Roma, Estradiol-17β-D-glucuronide induces endocytic internalization of Bsep in rats, Am. J. Physiol. (Gastrointest. Liver Physiol.) 285 (2003) G449–G459. https://doi.org/10.1152/ajpgi.00508.2002.

[36] A.C. Boaglio, A.E. Zucchetti, E.J. Sánchez Pozzi, J.M. Pellegrino, J.E. Ochoa, A.D. Mottino, M. Vore, F.A. Crocenzi, M.G. Roma, Phosphoinositide 3-kinase/protein kinase B signaling pathway is involved in estradiol 17β-D-glucuronide-induced cholestasis: Complementarity with classical protein kinase C, Hepatology 52 (2010) 1465–1476. https://doi.org/10.1002/hep.23846.

[37] F. A. Crocenzi, J.M. Pellegrino, V.A. Catania, M.G. Luquita, M.G. Roma, A.D. Mottino, E.J. Sánchez Pozzi, Galactosamine prevents ethinylestradiol-induced cholestasis, Drug Metab Dispos. 34 (2006): 993–997. https://doi.org/10.1124/dmd.106.009308.

[38] T. Yamada, M. Hoshino, T. Hayakawa, Y. Kamiya, H. Ohhara, K. Mizuno, H. Yamada, T. Nakazawa, T. Inagaki, A. Uchida, M. Miyaji, T.Takeuchi, Bile secretion in rats with indomethacin-induced intestinal inflammation, Am J Physiol (Gastrointest Liver Physiol.) 270 (1996): G804–G812. https://doi.org/10.1152/ajpgi.1996.270.5.g804.

[39] H. Yoshida , K. Okano, T. Tamano, Y. Kuronuma, M. Iijima, T. Harada, Bile flow in a mutant Sprague-Dawley rat with defective biliary excretion of glutathione, J. Gastroenterol. 29 (1994): 439–442. https://doi.org/10.1007/BF02361240.

[40] N. Ballatori, A.T. Truong, Glutathione as a primary osmotic driving force in hepatic bile formation, Am. J. Physiol. (Gastrointest. Liver Physiol.) 263 (1992) G617–G624. https://doi.org/10.1152/ajpgi.1992.263.5.g617.

[41] H.R. Kast, B. Goodwin, P.T. Tarr, S.A. Jones, A.M. Anisfeld, C.M. Stoltz, P. Tontonoz, S. Kliewer, T.M. Willson, P.A. Edwards, Regulation of multidrug resistance-

associated protein 2 (ABCC2) by the nuclear receptors pregnane X receptor, farnesoid X-activated receptor, and constitutive androstane receptor, J. Biol. Chem. 277 (2002) 2908–2915. https://doi.org/10.1074/jbc.M109326200.

[42] H.U. Marschall, M. Wagner, G. Zollner, P. Fickert, U. Diczfalusy, J. Gumhold, D. Silbert, A. Fuchsbichler, L. Benthin, R. Grundström, U. Gustafsson, S. Sahlin, C. Einarsson, M. Trauner, Complementary stimulation of hepatobiliary transport and detoxification systems by rifampicin and ursodeoxycholic acid in humans, Gastroenterology 129 (2005) 476–485. https://doi.org/10.1016/j.gastro.2005.05.009.

[43] L. Homolya, A. Váradi, B. Sarkadi, Multidrug resistance-associated proteins: Export pumps for conjugates with glutathione, glucuronate or sulfate, BioFactors 17 (2003) 103–114. https://doi.org/10.1002/biof.5520170111.

[44] I.M. Arias, L. Johnson, S. Wolfson, Biliary excretion of injected conjugated and unconjugated bilirubin by normal and Gunn rats, Am. J. Physiol. 200 (1961) 1091–1094. https://doi.org/10.1152/ajplegacy.1961.200.5.1091.

[45] J. Gollan, L. Hammaker, V. Licko, R. Schmid, Bilirubin kinetics in intact rats and isolated perfused liver. Evidence for hepatic deconjugation of bilirubin glucuronides, J. Clin. Invest. 67 (1981) 1003–1015. https://doi.org/10.1172/JCI110111.

[46] P.B. Miner, M. Sneller, S.S. Crawford, Spironolactone- and canrenone-induced changes in hepatic (Na^+, K^+)ATPase activity, surface membrane cholesterol and phospholipid, and fluorescence polarization in the rat, Hepatology 3 (1983) 481–488. https://doi.org/10.1002/hep.1840030403.

[47] J. Marrone, M. Danielli, C.I. Gaspari, R.A. Marinelli, Adenovirus-mediated human aquaporin-1 expression in hepatocytes improves lipopolysaccharide-induced cholestasis, IUBMB Life 69 (2017) 978–984. https://doi.org/10.1002/iub.1689.

[48] G.S. Miszczuk, I.R. Barosso, M.C. Larocca, J. Marrone, R.A. Marinelli, A.C. Boaglio, E.J. Sánchez Pozzi, M.G. Roma, F.A. Crocenzi, Mechanisms of canalicular transporter endocytosis in the cholestatic rat liver, Biochim. Biophys. Acta (Mol. Basis Dis.) 1864 (2018) 1072–1085. https://doi.org/10.1016/j.bbadis.2018.01.015.

[49] K. Yano, S. Sekine, K. Nemoto, T. Fuwa, T. Horie, The effect of dimerumic acid on LPS-induced downregulation of Mrp2 in the rat, Biochem. Pharmacol. 80 (2010) 533–539. https://doi.org/10.1016/j.bcp.2010.04.036.

[50] H. Murayama, A. Eguchi, M. Nakamura, M. Kawashima, R. Nagahara, S. Mizukami, M. Kimura, E. Makino, N. Takahashi, R. Ohtsuka, M. Koyanagi, S.-M. Hayashi, R.R. Maronpot, M. Shibutani, T. Yoshida, Spironolactone in combination with α-glycosyl isoquercitrin prevents steatosis-related early hepatocarcinogenesis in rats through the observed NADPH oxidase modulation, Toxicol. Pathol. 46 (2018) 530–539. https://doi.org/10.1177/0192623318778508.

[51] J.C.J. Pérez, A.C. Ramírez, L.T. González, L.E.M. Espinosa, M.M.P. Quintana, G.A. Galván, H.Z. Chavira, F.J.G. de la Garza, C.R.C. Lemarroy, N.E.F. Garza, E.P. Rodríguez, P.C. Pérez, Spironolactone effect in hepatic ischemia/reperfusion injury in Wistar rats, Oxid. Med. Cell. Longev. 2016 (2016) 3196431. https://doi.org/10.1155/2016/3196431.

[52] A. Duguay, I.M. Yousef, B. Tuchweber, G.L. Plaa, Alteration of lipid composition of hepatic membranes associated with manganese-bilirubin induced cholestasis, Fundam. Clin. Pharmacol. 12 (1998) 213–219. https://doi.org/10.1111/j.1472-8206.1998.tb00944.x.

[53] P.R. Mills, P.J. Meier, D.J. Smith, N. Ballatori, J.L. Boyer, E.R. Gordon, The effect of changes in the fluid state of rat liver plasma membrane on the transport of taurocholate, Hepatology 7 (1987) 61–66. https://doi.org/10.1002/hep.1840070114.

[54] S. Yasumiba, S. Tazuma, H. Ochi, K. Chayama, G. Kajiyama, Cyclosporin A reduces canalicular membrane fluidity and regulates transporter function in rats, Biochem. J. 354 (2001) 591–596. https://doi.org/10.1042/0264-6021:3540591.

[55] R. Salgia, J.H. Becker, M.M. Sayeed, Altered membrane fluidity in rat hepatocytes during endotoxic shock, Mol. Cell. Biochem. 121 (1993) 143–148. https://doi.org/10.1007/BF00925973.

[56] S. Patel, A. Rauf, H. Khan, T. Abu-Izneid, Renin-angiotensin-aldosterone (RAAS): The ubiquitous system for homeostasis and pathologies, Biomed. Pharmacother. 94 (2017) 317–325. https://doi.org/10.1016/j.biopha.2017.07.091.

Table 1. Sequence of primers used in Real-time PCR.

Gen target	Primer	Primer sequence (5' → 3')
Bsep	Forward	CCGAAGGCTCAGGGTATTGG
	Reverse	ATCAGGTGACATGGTGGCAG
Mrp2	Forward	ACCTTCCACGTAGTGATCCT
	Reverse	ACCTGCTAAGATGCACGGTC
18s rRNA	Forward	GTAACCCGTTGAACCCCATT
	Reverse	CCATCCAATCGGTAGTAGCG

Table 2. Basal biliary parameters.

	Control	SL	LPS	SL+LPS
BF (µl/min per g liver)	3.5 ± 0.1	3.9 ± 0.2	2.4 ± 0.1*	3.1 ± 0.2$^{\#}$
TBA output (nmol/min per g liver)	52 ± 8	43 ± 7	31 ± 3*	30 ± 4*
Total GSH output (nmol/min per g liver)	1.35 ± 0.11	1.71 ± 0.24	0.37 ± 0.05*	0.76 ± 0.12*$^{\#}$
BSIBF (µl/min per g liver)	3.0 ± 0.3	3.6 ± 0.2	1.9 ± 0.1*	2.8 ± 0.1$^{\#}$

BF, bile flow; BSIBF; bile salt independent bile flow; GSH, glutathione; LPS, lipopolysaccharide; SL, spironolactone; TBA, total bile acids.

*P < 0.05 *vs.* control; $^{\#}$P < 0.05 *vs.* LPS. *n* = 3-15.

Table 3. Serum biochemical parameters.

	Control	SL	LPS	SL+LPS
ALP (U/l)	370 ± 24	402 ± 43	535 ± 56*	516 ± 68*
AST (U/l)	135 ± 16	113 ± 11	145 ± 27	168 ± 23
ALT (U/l)	42 ± 16	35 ± 7	41 ± 16	28 ± 7
LDH (U/l)	381 ± 29	364 ± 24	559 ± 119	640 ± 197

ALP, alkaline phosphatase; AST, aspartate aminotransferase; ALT, alanine aminotransferase; LDH, lactate dehydrogenase; LPS, lipopolysaccharide; SL, spironolactone; TBA, total bile acids.

*P < 0.05 *vs.* control; #P < 0.05 *vs.* LPS. *n* = 4-13.

Table 4. TC-stimulated biliary parameters.

	Control	SL	LPS	SL+LPS
TC-stimulated† BF (µl/min per g liver)	5.8 ± 0.1	5.5 ± 0.1	3.4 ± 0.1*	4.3 ± 0.1*#
TC-stimulated† TBA output (nmol/min per g liver)	237 ± 17	212 ± 37	129 ± 9*	151 ± 3*

BF, bile flow; LPS, lipopolysaccharide; SL, spironolactone; TC, taurocholate; TBA, total bile acids.

†TC-stimulated values correspond to the maximum value obtained after a TC i.v. injection of 8 µmol/100 g of b.w.

*P < 0.05 *vs.* control; #P < 0.05 *vs.* LPS. *n* = 3-4.

Table 5. Mrp2 and Bsep mRNA expression by Real-time PCR.

mRNA levels (% of mean control values)	Control	SL	LPS	SL+LPS
Mrp2	100 ± 6	145 ± 2*	64 ± 5*	85 ± 6$^{\#}$
Bsep	100 ± 12	82 ± 11	39 ± 3*	36 ± 2*

LPS, lipopolysaccharide; SL, spironolactone.

*P < 0.05 *vs.* control; $^{\#}$P < 0.05 *vs.* LPS. *n* = 3-7.

Table 6. Plasma levels of pro-inflammatory cytokines IL-1β, TNF-α, and IL-6.

Pro-inflammatory cytokines	Control	SL	LPS	SL+LPS
IL-1β (pg/mL)	190 ± 44	198 ± 45	648 ± 78*	517 ± 61*
TNF-α (pg/mL)	13 ± 1	8 ± 1	30 ± 9	17 ± 1*
IL-6 (pg/mL)	108 ± 24	129 ± 35	2130 ± 222*	1685 ± 101*

IL-1β, interleukin-1β; IL-6, interleukin-6; LPS, lipopolysaccharide; SL, spironolactone TNF-α, tumor necrosis factor-α.

*P < 0.05 *vs.* control; #P < 0.05 *vs.* LPS. *n* = 3-4.

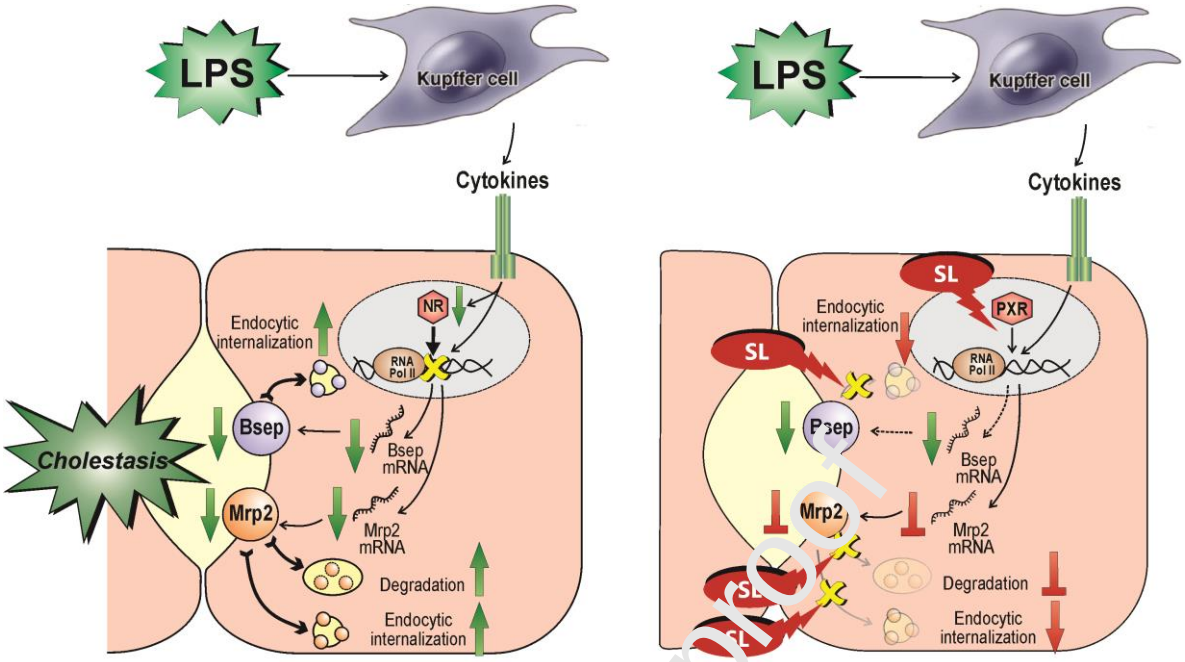

Graphical abstract